

MHz): δ 0.90 [3 H, t, $-\text{OC}(\text{O})\text{CH}_2\text{CH}_2\text{CH}_3$], 1.55 [2 H, sextet, $-\text{OC}(\text{O})\text{CH}_2\text{CH}_2\text{CH}_3$], 2.28 [2 H, t, $-\text{OC}(\text{O})\text{CH}_2\text{CH}_2\text{CH}_3$], 1.55 (1 H, m, H2 α), 1.85 (1 H, dd, H5 α), 1.95 (1 H, dd, H8 α), 2.02 (1 H, ddd, H3 α), 2.23 (1 H, m, H2 β), 2.98 (1 H, dt, H3 β), 3.05 (1 H, dd, H5 β), 3.28 (1 H, dd, H7), 3.47 (1 H, dd, H8), 3.65 (2 H, s, $-\text{OC}(\text{O})\text{CH}_2\text{C}_6\text{H}_5$), 4.62 (1 H, ddd, H6), 5.15 (1 H, m, H1), 7.25-7.35 (5 H, aromatic). MS: m/e 378 (MH⁺), 360 (MH⁺ - H₂O), 290 [MH⁺ - HOC(O)-CH₂CH₂CH₃], 242 [MH⁺ - H(O)COCH₂C₆H₅]. Anal. Calcd for C₂₀H₂₇O₆N: C, 63.63; H, 7.21; N, 3.71. Found: C, 63.27; H, 7.28; N, 3.71.

Enzymatic Synthesis of 1-O-(Phenylacetyl)-7-O-butryl-castanospermine. Chromatography with 5% EtOH/CH₂Cl₂ (*R_f* 0.15) resulted in an oil. ¹H NMR (DMSO-*d*₆, 300 MHz): δ 0.92 [3 H, t, $-\text{OC}(\text{O})\text{CH}_2\text{CH}_2\text{CH}_3$], 1.60 [2 H, sextet, $-\text{OC}(\text{O})\text{CH}_2\text{CH}_2\text{CH}_3$], 2.32 [2 H, t, $-\text{OC}(\text{O})\text{CH}_2\text{CH}_2\text{CH}_3$], 1.55 (1 H, m, H2 α), 1.88 (1 H, dd, H5 α), 2.02 (1 H, dd, H8 α), 2.05 (1 H, ddd, H3 α), 2.25 (1 H, m, H2 β), 2.98 (1 H, dt, H3 β), 3.05 (1 H, dd, H5 β), 3.50 (1 H, t, H8), 3.52 (1 H, dt, H6), 3.65 (2 H, s, $-\text{OC}(\text{O})\text{CH}_2\text{C}_6\text{H}_5$), 4.57 (1 H, t, H7), 5.12 (1 H, m, H1), 7.25-7.35 (5 H, aromatic). MS: m/e 378 (MH⁺), 360 (MH⁺ - H₂O), 290 [MH⁺ - HOC(O)-CH₂CH₂CH₃], 242 [MH⁺ - HOC(O)-CH₂C₆H₅]. Anal. Calcd for C₂₀H₂₇O₆N: C, 63.63; H, 7.21; N, 3.71. Found: C, 63.30; H, 7.37; N, 3.39.

Enzymatic Synthesis of 1-O-Butyryl-7-O-(phenylacetyl)castanospermine. Chromatography with 3.5% EtOH/CH₂Cl₂ (*R_f* 0.30) resulted in a waxy semisolid. ¹H NMR (DMSO-*d*₆, 300 MHz): δ 0.92 [3 H, t,

$-\text{OC}(\text{O})\text{CH}_2\text{CH}_2\text{CH}_3$], 1.58 [2 H, sextet, $-\text{OC}(\text{O})\text{CH}_2\text{CH}_2\text{CH}_3$], 2.31 [2 H, t, $-\text{OC}(\text{O})\text{CH}_2\text{CH}_2\text{CH}_3$], 1.55 (1 H, m, H2 α), 1.88 (1 H, dd, H5 α), 2.00 (1 H, dd, H8 α), 2.02 (1 H, quartet, H3 α), 2.25 (1 H, m, H2 β), 2.98 (1 H, dt, H3 β), 3.04 (1 H, dd, H5 β), 3.51 (1 H, t, H8), 3.52 (1 H, dt, H6), 3.65 [2 H, s, $-\text{OC}(\text{O})\text{CH}_2\text{C}_6\text{H}_5$], 4.62 (1 H, t, H7), 5.14 (1 H, m, H1), 7.25-7.35 (5 H, aromatic). MS: m/e 378 (MH⁺), 360 (MH⁺ - H₂O), 290 [MH⁺ - HOC(O)-CH₂CH₂CH₃], 242 [MH⁺ - HOC(O)-CH₂C₆H₅]. HRMS (CI, CH₄ as ionizing gas) for C₂₀H₂₈O₆N (M⁺ + 1): calcd 378.1838, found 378.1917.

Enzymatic Synthesis of 1-O-Butyryl-6-O-(phenylacetyl)castanospermine. Chromatography with 3.5% EtOH/CH₂Cl₂ (*R_f* 0.37) resulted in a waxy semisolid. ¹H NMR (DMSO-*d*₆, 300 MHz): δ 0.88 [3 H, t, $-\text{OC}(\text{O})\text{CH}_2\text{CH}_2\text{CH}_3$], 1.52 [2 H, sextet, $-\text{OC}(\text{O})\text{CH}_2\text{CH}_2\text{CH}_3$], 2.22 [2 H, t, $-\text{OC}(\text{O})\text{CH}_2\text{CH}_2\text{CH}_3$], 1.52 (1 H, m, H2 α), 1.85 (1 H, dd, H5 α), 1.95 (1 H, dd, H8 α), 2.02 (1 H, ddd, H3 α), 2.22 (1 H, m, H2 β), 2.95 (1 H, dt, H3 β), 3.05 (1 H, dd, H5 β), 3.28 (1 H, m, H7), 3.4 (1 H, dd, H8), 3.65 [1 H, s, $-\text{OC}(\text{O})\text{CH}_2\text{C}_6\text{H}_5$], 4.62 (1 H, ddd, H6), 5.08 (1 H, m, H1), 7.25-7.35 (5 H, aromatic). MS: m/e 378 (MH⁺), 360 (MH⁺ - H₂O), 242 [MH⁺ - HOC(O)-CH₂C₆H₅], 137. HRMS (CI, CH₄ as ionizing gas) for C₂₀H₂₈O₆N (M⁺ + 1): calcd 378.1838; found 378.1917.

Acknowledgment. We are grateful to Gary Ruba for his assistance with analytical data and to Dr. Jack Martin for helpful discussions and encouragement.

MSX α Study of Absorption Spectra of Free Radicals. Characterization of Rydberg and Valence Transitions in Alkyl Derivatives of Group 14 Centered Radicals

C. Chatgililoglu and M. Guerra*

Contribution from the Istituto dei Composti del Carbonio Contenenti Eteroatomi e loro Applicazioni, CNR, Via della Chimica 8, 40064 Ozzano Emilia, Bologna, Italy.
Received December 15, 1988

Abstract: Ionization potentials, electronic transition energies, and oscillator strengths were computed by the MSX α method for methyl, ethyl, isopropyl, *tert*-butyl, and X₃M* radicals (M = Si, Ge, Sn; X = H, CH₃). The best procedure, within the MSX α framework, for assigning optical absorption spectra in radicals was established. In alkyl and H₃M* radicals, the transition energies are in very good agreement with experiment and available ab initio CI calculations. The optical spectra of alkyl derivatives of heteroatom-centered radicals are assigned for the first time. The low-lying transitions are predominantly Rydberg in character and are red shifted as the degree of alkyl substitution increases or the electronegativity of the central atom M decreases in accordance with the trend of the vertical ionization potentials. In heteroatom-centered radicals, the first valence transition from the M-C bond to SOMO is strongly red shifted and occurs in the range of the lowest Rydberg transitions.

Short-lived radicals and their chemical behavior are usually investigated by optical detection techniques. In spite of the large number of electronic absorption spectra of free radicals reported in the literature, information on the nature of optical transitions is scarce.¹ For example, although the ultraviolet absorption of the methyl radical was assigned over 30 years ago, due to the work of Herzberg,² only recently have the electronic spectra of other simple alkyl radicals been characterized³ and understood by means of ab initio calculations.⁴ However, the most accurate theoretical methods, which involve some form of configuration interaction (CI), are prohibitive for the interpretation of electronic properties

of large radicals or radicals containing heavy atoms.

The multiple scattering X α (MSX α) method could be a powerful tool for assigning optical transitions in radicals.⁵ As opposed to traditional LCAO methods, it requires little computational effort, so that large polyatomic systems can be investigated, and it treats, at the same level of accuracy, both valence excited and Rydberg states owing to the radial flexibility of the wave functions. It is well established that the MSX α method satisfactorily describes the electronic properties of molecules in ground and valence excited states. Indeed, ionization potentials,⁶ electron affinities,⁷ and electronic transitions⁸ are reproducible with an accuracy comparable with LCAO-CI calculations with extended basis sets.

In this work, we have studied a number of group 14 centered radicals to see if the MSX α method can correctly predict electronic

(1) For a recent collection of optical spectral parameters of neutral free radicals, see: Chatgililoglu, C. *Handbook of Organic Photochemistry*; Scaiano, J. C., Ed.; CRC Press: Boca Raton, FL, 1989; Part IV, Section 1.

(2) Herzberg, G. *Proc. R. Soc. London*, **A 1961**, *262*, 291. Herzberg, G. *Molecular Spectra and Molecular Structure. III. Electronic Spectra and Electronic Structure of Polyatomic Molecules*; Van Nostrand Reinhold: New York, 1966.

(3) Wendt, H. R.; Hunziker, H. E. *J. Chem. Phys.* **1984**, *81*, 717.

(4) Lengsfeld, B. H., III.; Siegbahn, P. E. M.; Liu, B. *J. Chem. Phys.* **1984**, *81*, 710.

(5) Chatgililoglu, C.; Griller, D.; Guerra, M. *J. Phys. Chem.* **1987**, *81*, 3747.

(6) De Alti, G.; Decleva, P.; Lisini, A. *Chem. Phys.* **1982**, *66*, 425.

(7) Guerra, M.; Jones, D.; Distefano, G.; Foffani, A.; Modelli, A. *J. Am. Chem. Soc.* **1988**, *110*, 375.

(8) Roberge, R.; Salahub, D. R. *J. Chem. Phys.* **1979**, *70*, 1177.

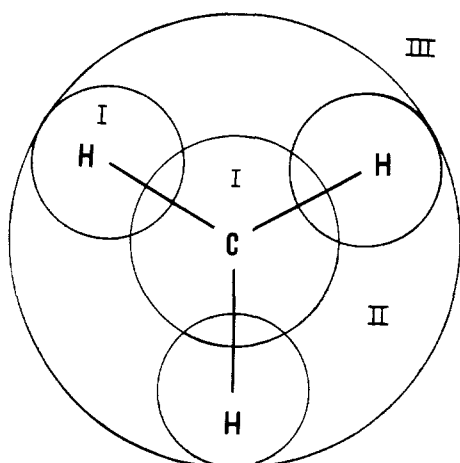


Figure 1. Division of space in the scattered-wave method into atomic (I), intersphere (II), and extramolecular (III) regions for the methyl radical.

properties of radicals, such as ionization potentials and optical transitions to excited states that could be multicenter (valence excited states) or one center (Rydberg states) in character. First, the best MSX α procedure for studying optical transitions in radicals will be established by performing different types of MSX α calculations on alkyl radicals and H₃M^{*}. The results will be compared with experiment and previous LCAO calculations. The optical absorption spectra of alkyl derivatives of group 14 heteroatom-centered radicals,⁹ viz., (alkyl)₃M^{*} (M = Si, Ge, Sn), will be then assigned, and the influence of the electronic nature of the heteroatom on the transition energies will be discussed.

Method and Computational Details

A detailed description of the MSX α procedure can be found in Johnson's review,¹⁰ and only a brief description of the method is reported here.

In the X α theory,¹¹ the molecular orbitals are solutions of a set of one-electron differential equations (in atomic units).

$$[-\frac{1}{2}\nabla^2 + V_c(1) + V_{xc}(1)]\psi(1) = \epsilon\psi(1) \quad (1)$$

V_c is the normal coulomb potential, and V_{xc} is an approximate potential representing the exchange-correlation potential. This is related to the local electronic charge density ρ and a scaling factor α .

$$V_{xc} = -6\alpha[\frac{3}{8}\pi\rho(r)]^{1/3} \quad (2)$$

The multiple scattering procedure allows the efficient solution of eq 1. In this approach, the coordinate space of the molecule is partitioned into three regions as shown for the methyl radical in Figure 1: (i) Atomic regions I are inside the spheres centered on the atoms. The potential is assumed to be spherically symmetric. (ii) Intersphere region II is the region between the atomic spheres and an outer sphere surrounding the entire molecule. In this intersphere region the potential is taken to be a constant, determined by the volume average of the potential. (iii) Extramolecular region III is the region in which the potential is also assumed to be spherically symmetric. To circumvent the limitations that result from the assumption of a constant potential in the intersphere region, the atomic spheres are usually allowed to partially overlap.¹²

In the atomic (I) and outer-sphere (III) regions the electronic wave function is expanded in the form

$$\psi_j^l(r) = \sum_L C_L^j R_l^j(\epsilon_j, r) Y_L^j(r) \quad (j = I, III) \quad (3)$$

where $L = (l, m)$ is the partial wave index, C_L^j are coefficients to be determined, R_l^j are the numerical solutions of the radial part of eq 1 for each partial wave component l and trial values of the energy ϵ_j , and Y_L^j are real spherical harmonics. Thus, the radial wave functions correspond to saturated LCAO basis functions for each partial wave L employed in the expansion of the wave function inside the atomic spheres. The difficulty, present in LCAO methods, of choosing an analytical basis set that adequately describes both valence and Rydberg orbitals is then avoided.

(9) Chatgililoglu, C.; Ingold, K. U.; Luszyk, J.; Nazran, A. S.; Scaiano, J. C. *Organometallics* **1983**, *2*, 1332.

(10) Johnson, K. H. *Adv. Quantum Chem.* **1973**, *7*, 143.

(11) Slater, J. C. *Adv. Quantum Chem.* **1972**, *6*, 1.

(12) Herman, F.; Williams, A. R.; Johnson, K. H. *J. Chem. Phys.* **1974**, *61*, 3508.

In the intersphere region, a multicenter expansion of the wave function is used. The expansion coefficients are determined by solving a set of homogeneous linear equations under the condition that the wave function and its first derivative are continuous at the sphere boundaries. The energy-dependent numerical orbitals depend only on the potential and not on the basis set; therefore, imaginary excited states that appear in the LCAO approach when basis functions are added to a minimal basis set to better describe molecular properties do not occur in the scattered-wave approach.⁸ According to the geometrical decomposition of the coordinate space, the resulting molecular orbitals may be classified as either multiple center (valence-like) or single center (Rydberg-like), depending on the relative charge computed inside the atomic spheres and outside the outer sphere.

The orbital eigenvalues ϵ_i are not related to ionization potentials or electron affinities through the Koopmans' theorem¹³ as in Hartree-Fock theory, but to the X α statistical total energy ($E_{X\alpha}$) as the first derivatives of the total energy with respect to the orbital occupation number n_i :

$$\epsilon_i = \partial(E_{X\alpha})/\partial n_i \quad (4)$$

Slater introduced the transition-state concept for computing electronic energies of excited states utilizing this equation.¹⁴ The energy variation occurring in an electronic process is approximately equal to the difference between the one-electron energies orbitals whose occupation numbers are halfway between those of the initial and final electronic states. Hence, the relaxation effects that occur in the excitation process are taken into account as in the more traditional Δ SCF procedure.

MSX α calculations in both non-spin-polarized (NSP) and spin-polarized (SP) forms were performed on the methyl, ethyl, isopropyl, *tert*-butyl, and X₃M^{*} radicals (M = Si, Ge, Sn; X = H, CH₃). For H₃Sn^{*}, scalar relativistic calculations¹⁵ were also carried out. The geometrical parameters for alkyl radicals were taken from ref 4, for H₃M^{*} from ref 16, and for the trimethylsilyl radical from ref 17. For trimethylgermyl and trimethyltin radicals neither experimental nor theoretical structural parameters are available, and then they are assumed to have the same degree of pyramidalization^{16,18,20,21,25} as the silyl analogue and standard bond lengths.²⁶

The local exchange parameters α were taken from the tabulation of Schwarz.²⁷ The radii ratios for the atomic spheres were determined with the nonempirical method of Norman.²⁸ As far as the atomic sphere radii are concerned, both touching (TS) and overlapping (OS) spheres are used. In the latter case, the sphere radii were changed until the virial ratio of total kinetic T and potential V energies satisfied the virial con-

(13) Koopmans, T. A. *Physica* **1933**, *1*, 104.

(14) Slater, J. C. *Computational Methods in Band Theory*; Plenum Press: New York, 1971.

(15) Koelling, D. D.; Harmon, B. N. *J. Phys. C* **1977**, *10*, 3107.

(16) Selmani, A.; Salahub, D. R. *Chem. Phys. Lett.* **1988**, *146*, 465.

(17) Cartledge, F. K.; Piccione, R. V. *Organometallics* **1984**, *3*, 299.

(18) Gordy and co-workers experimentally determined that H₃C^{*} is planar while the degree of pyramidality is very similar in H₃Si^{*} and H₃Ge^{*}, with out-of-plane angles of 15.1° and 13.1°, respectively.¹⁹

(19) Morehouse, R. L.; Christiansen, J. J.; Gordy, W. *J. Chem. Phys.* **1966**, *45*, 1751. Jackel, G. S.; Christiansen, J. J.; Gordy, W. *J. Chem. Phys.* **1967**, *47*, 4274. Jackel, G. S.; Gordy, W. *Phys. Rev.* **1968**, *176*, 443.

(20) A qualitative consideration based on the electrostatic force theory suggests that the out-of-plane angle will increase as the central atom becomes heavier in the group 14 elements, the gap being large between C and Si and small among Si, Ge, and Sn. See: Nakatsuji, H. *J. Am. Chem. Soc.* **1973**, *95*, 345.

(21) Triorganosilyl, -germyl, and -stannyl radicals are approximately tetrahedral and when generated from optically active precursors can yield products that are optically active and have retained the configuration of starting material.²² Rate constants for the inversion of (1-naphthyl)phenylmethylsilyl²³ and -germyl²⁴ radicals have been estimated to be 6.8×10^9 and 1.0×10^9 s⁻¹, respectively, at 80 °C.

(22) For a review on this problem, see: Beckwith, A. L. J.; Ingold, K. U. *Rearrangements in Ground and Excited States*; de Mayo, P., Ed.; Academic Press: New York, 1980; Vol. 1, Essay No. 4.

(23) Chatgililoglu, C.; Ingold, K. U.; Scaiano, J. C. *J. Am. Chem. Soc.* **1982**, *104*, 5123.

(24) Ingold, K. U.; Luszyk, J.; Scaiano, J. C. *J. Am. Chem. Soc.* **1984**, *106*, 343.

(25) Further evidence in this direction comes from ESR data. For example, see: Lehnig, M.; Neumann, W. P.; Wallis, E. J. *Organomet. Chem.* **1987**, *333*, 17, and references therein.

(26) *Tables of Interatomic Distances*; Sutton, L. E., Ed.; The Chemical Society: London, 1958.

(27) Schwarz, K. *Phys. Rev. B* **1972**, *5*, 2466; *Theor. Chim. Acta* **1974**, *34*, 225.

(28) Norman, J. G., Jr. *J. Chem. Phys.* **1974**, *61*, 1974.

Table I. Vertical Transition Energies (cm^{-1}) and Vertical Ionization Potentials (eV) for the Methyl Radical ($\text{X}^2\text{A}_2''$)^a (Oscillator Strengths Reported in Parentheses)

	MSX α -TS ^b	MSX α -OS ^c	MSX α -SP	MSX α -DC	CI ^d	exptl
$^2\text{A}_1'(3s)$	60 900 (0.019)	40 100 (0.026)	40 500 (0.026)	44 000 (0.019)	45 940	46 205 ^e
$^2\text{E}'(3p)$	73 000 (0.000)	49 900 (0.000)	50 500 (0.000)	54 900 (0.000)	55 630	
$^2\text{A}_2''(3p)$	73 200 (0.000)	50 300 (0.000)	50 900 (0.000)	55 700 (0.000)	57 550	59 925 ^f
$^2\text{E}''(3d)$	78 300 (0.000)	58 000 (0.000)	59 000 (0.000)	63 000 (0.000)		
$^2\text{A}_1'(3d)$	78 300 (0.054)	58 100 (0.014)	59 100 (0.014)	63 100 (0.014)		66 799 ^e
$^2\text{E}''(3d)$	80 600 (0.008)	58 400 (0.004)	59 500 (0.004)	63 400 (0.004)	64 151	66 536 ^e
$^2\text{E}'(\text{val})$	35 500 (0.000)	54 500 (0.000)	54 200 (0.000)	58 900 (0.000)	59 488	
IP	11.3	8.4	9.0	9.4 ^g	9.45	9.84 ^h

^a MSX α procedure: The sphere radii are $r_C = 1.2123$, $r_H = 0.8287$, and $r_{\text{out}} = 2.8697$ for touching spheres (TS); $r_C = 1.6845$, $r_H = 1.1516$, and $r_{\text{out}} = 3.1926$ for overlapping spheres (OS), and spin polarized (SP); $r_C = 1.6971$, $r_H = 1.1602$, and $r_{\text{out}} = 3.2012$ for double counting (DC); for more details see text. ^b Virial ratio is 1.016. ^c Overlap (%) of the sphere volume is 33.2 for C and 34.8 for H, respectively. ^d From ref 4. ^e From ref 2. ^f From ref 30. ^g Spin-unrestricted value; restricted value is 8.8 eV. ^h From ref 32.

dition $-2T/V = 1$. Core electrons were not frozen during the SCF procedure, and the potential converged to better than 1.0×10^{-4} at any point. The ionization potentials IP and the optical transition energies were evaluated by with Slater's transition-state method. The oscillator strengths were computed in the acceleration form within the scattered-wave framework.²⁹ Wave functions were expanded in partial waves up to $l = 0$ (s), $l = 1$ (sp), $l = 2$ (spd), and $l = 3$ (spdf) in the hydrogen, carbon, central atom, and outer spheres, respectively. The outer-sphere center was located at the barycenter of the valence electrons.

Since the energies of Rydberg orbitals are often positive for the ground-state potential, the excitation energies were evaluated starting from the transition-state potential used for computing the ionization potential, which has bound excited orbitals because Rydberg states converge to the ionic limit.

The calculations were performed on the FPS array processor attached to the VAX 11/780 computer of the Theoretical Chemistry Group in Bologna.

Results and Discussion

Methyl Radical. We carried out four types of MSX α calculations on methyl, the simplest alkyl radical, in order to determine the best procedure within the MSX α framework for studying optical spectra of alkyl radicals. Experimental evidence and theoretical calculations indicate a planar D_{3h} structure for methyl, and optical transitions have been characterized by one-photon² [$\text{X}^2\text{A}_2'' \rightarrow ^2\text{A}_1'(3s)$, $^2\text{E}''(3d)$, $^2\text{A}_1'(3d)$] spectroscopy, two-photon³⁰ [$\text{X}^2\text{A}_2'' \rightarrow ^2\text{A}_2''(3p)$] spectroscopy, and accurate ab initio CI calculations.⁴ In the first procedure (TS), the atomic sphere radii were kept tangential to each other; in the second one (OS), the atomic spheres were allowed to overlap, the degree of overlap being determined by the virial ratio criterion; in the third one (SP), the spin-coupled constraint was released; and in the last procedure (DC), the electronic charge within the atomic spheres was normalized with the double-counting correction proposed by Herman,³¹ which avoids assigning the electronic charge in the overlap region to both the atomic spheres simultaneously. The results of the MSX α calculations are summarized in Table I together with experimental and LCAO results. The calculated oscillator strengths are utilized to characterize the one-photon transitions.

The present calculations, in agreement with CI calculations, show that low-lying transitions occur from the 2p orbital of the carbon atom (SOMO) to orbitals that are Rydberg in character. In fact, in these orbitals more than 90% of the electronic charge resides outside the outer sphere (see Table II). Multiplet splittings of the 3p and 3d Rydberg states are relatively small compared with the separation of 3s, 3p, and 3d states. A valence excitation from the highest occupied orbital to SOMO was also computed at low energy. Although the experimental value for this valence transition is not available, since the allowed multiphoton transition [$\text{X}^2\text{A}_2'' \rightarrow ^2\text{E}'$] was not determined experimentally, its transition energy was evaluated with an accurate CI calculation. We utilized this transition to evaluate the suitability of the MSX α method

Table II. Charge Distributions (%) in the Rydberg Orbitals for the Methyl Radical

orbital	C	H	int	out
a'(3s)	3	0	4	93
e'(3p)	1	0	1	98
a''(3p)	2	0	1	97
e'(3d)	0	0	1	99
a'(3d)	1	0	1	98
e''(3d)	0	0	1	99
SOMO	55	0	36	9

for reproducing the transition energy of excitations that are different in nature. The ordering of the Rydberg transitions is the same for each procedure, the transition energies being uniformly shifted. On the other hand, some caution has to be used when comparing valence and Rydberg excitation energies computed with the TS approach. This procedure leads to energies of Rydberg transitions that are systematically too large by about $15\,000 \text{ cm}^{-1}$ with respect to experiment and CI calculations with the valence transition $24\,000 \text{ cm}^{-1}$ lower in energy than in the CI calculation. As far as the oscillator strength is concerned, the values computed for the allowed Rydberg transitions are less than 0.1 as expected for this type of transition³³ and are not significantly affected when the MSX α procedure is changed, their trend being the same. They can thus be used as a guide to assign optical spectra.

The discrepancies in the excitation energies decrease when the spheres are allowed to overlap (OS). The deviation from experiment decreases to about $8\,000 \text{ cm}^{-1}$ in the excitation energies, and both valence and Rydberg transitions are in agreement with the CI results, being lower in energy by $4\,700$ and about $6\,000 \text{ cm}^{-1}$, respectively. A large difference, about 1.4 eV ($11\,300 \text{ cm}^{-1}$), remains in the ionization potential. However, spin correlation effects, which could affect the electronic properties of radicals, were not taken into account. In spin-polarized calculations (SP) the ionization potential increases significantly by about 0.6 eV whereas variations in the optical transition energies are less than $1\,000 \text{ cm}^{-1}$ and the oscillator strengths are left unchanged. Indeed, only in the photoionization process is there a change in the total number of "spin-up" electrons, which causes a sizable variation in the difference between the polarized exchange-correlation potential V_{xc} of the initial and final states. As regards Rydberg transitions, a similar variation is expected for states having high principal quantum number. The small shift due to spin polarization computed for the Rydberg excitation energies probably means that the electron density of the first Rydberg states is rather localized. However, the shift increases with the excitation energy, then converging correctly to the ionic limit. Hence MSX α -SP calculations are necessary only for computing ionization potentials in radicals.³⁴ Other exchange-correlation potentials,^{36,37} which

(29) Noodelman, L. *J. Chem. Phys.* **1976**, *64*, 2343.(30) Hudgens, J. W.; DiGiuseppe, T. G.; Lin, M. C. *J. Chem. Phys.* **1983**, *79*, 571.(31) Herman, F. *Electrons in Finite and Infinite Structures*; Phariseau, P., Scheire, L., Eds.; Plenum Press: New York, 1977.(32) Houle, F. A.; Beauchamp, J. L. *J. Am. Chem. Soc.* **1979**, *101*, 4067.(33) Robin, M. B. *Higher Excited States of Polyatomic Molecules*; Academic Press: New York, 1974; Vol. 1.(34) Similar results have been recently obtained³⁵ for the calculated ionization potentials of X_3C^+ , where X = F, Cl, and Br, with MSX α approach. That is, the spin-polarized ionization potentials are higher than the non-spin-polarized ones by $0.3\text{--}0.4 \text{ eV}$.

Table III. Vertical Transition Energies (cm⁻¹), Vertical Ionization Potentials (eV), and Charge Distributions in the Excited Orbitals for the Ethyl Radical (\dot{X}^2A') (Oscillator Strengths Reported in Parentheses)

	exptl	CI ^a	MSX α -DC ^b	% charge distribution				
				C	H	Me	int	out
$^2A'(3s)$	40 600 ^c	41 460	33 800 (0.077)	2	0	2	17	79
$^2A'(3p)$	48 800 ^c	47 850	41 100 (0.006)	2	0	1	5	92
$^2A''(3p)$		48 517	41 200 (0.001)	1	0	1	6	92
$^2A'(3p)$		49 566	42 700 (0.001)	1	0	1	2	96
$^2A'(3d)$			48 300 (0.023)	1	0	1	4	94
$^2A''(3d)$		56 421	48 600 (0.010)	0	0	0	4	96
$^2A'(3d)$			50 600 (0.000)	1	0	0	0	99
$^2A''(3d)$			50 700 (0.000)	1	0	0	0	99
$^2A'(3d)$			50 900 (0.002)	0	0	0	1	99
$^2A'(val)$		57 079	56 400 (0.015)	35	10	41	11	3
IP	8.50 ^d	8.41	7.9 ^e	56	0	7	33	4

^a From ref. 4. ^b The sphere radii are $r_{C\alpha} = 1.7577$, $r_{C\beta} = 1.6890$, $r_H = 1.2269$, and $r_{out} = 4.3148$. ^c From ref. 3. ^d From ref. 32. ^e SP value; spin-restricted value is 7.5 eV.

are more correlated than the one employed herein, have been used in local spin density calculations rather than in the MSX α methodology. However, the test of these potentials is beyond the target of the present work.

In previous MSX α studies on ionization potentials and electron affinities,⁷ we found that the electronic properties were better reproduced if the double-counting correction (DC) in normalizing the molecular orbitals was employed. Indeed, the agreement between transition energies and optical spectrum improves in the DC procedure. Table I shows that the accuracy of the MSX α calculations (3500 cm⁻¹) becomes comparable to that of CI calculations (2000 cm⁻¹).

Other Alkyl Radicals. In the other alkyl radicals examined, the computed transition energies follow the behavior of the methyl radical when the MSX α procedure is changed. Therefore, we will discuss only the MSX α results computed with the DC procedure. In the ethyl radical the substitution of a hydrogen atom with a methyl group produces structural and electronic effects. The symmetry of the radical is reduced from D_{3h} to C_s , the radical center no longer being planar, and the experimental electronic transitions are red shifted.⁴ The MSX α -DC calculations, reported in Table III, reproduce the ordering of the Rydberg transitions as well as the observed red shift. However, the transition energies are underestimated by about 7500 cm⁻¹. A significant deviation (6000 cm⁻¹) was also obtained for the isopropyl radical (C_s symmetry) (see Table IV). On the other hand, in the *tert*-butyl radical (C_{3v} symmetry) the agreement with experiment becomes slightly better than in methyl, the difference falling to about 2000 cm⁻¹ (see Table V). Two factors could be responsible for this different behavior: (i) the lowering of symmetry on going from methyl and *tert*-butyl to ethyl and isopropyl that causes the approximation of the potential averaging in the atomic spheres to become inadequate and (ii) the greatest increase of the intersphere volume with respect to the atomic sphere volume in symmetric radicals that produces an underestimation of the constant potential. That is, a large part of the intersphere region on the side of the hydrogens attached to the central atom in partially substituted methyl radicals should have low electron density but should contribute to the average intersphere potential.³⁹ Nevertheless, the red shift caused by the replacement of a hydrogen with a methyl group

is well reproduced along the alkyl series by the MSX α -DC calculations.

As far as the first valence transition is concerned, the agreement with the CI calculation is excellent for methyl, ethyl, and isopropyl radicals, probably because the electronic charge density in the orbitals involved in the transition is predominantly located inside the atomic spheres, and this supports the above point ii. In the *tert*-butyl radical the MSX α -DC value for the valence transition is 8500 cm⁻¹ lower than the SCF value. Unfortunately, CI calculations are not available for the assignment of the UV spectrum of the *tert*-butyl radical, although it is known that the SCF method overestimates the valence transition with respect to the CI approach in the other alkyl radicals.⁴ Furthermore, the first valence transition in the region of ca. 59 000 cm⁻¹ in methyl is red shifted in all the substituted methyl radicals, in agreement with the expected increasing stability of the SOMO.

Heteroatom-Centered Radicals. We have found that the MSX α -DC approach gives results that are in excellent agreement with experiment in highly symmetric alkyl radicals such as methyl and *tert*-butyl. In order to study the effect of heteroatoms on the excitation energies, we have examined the analogues of group 14 centered radicals.

The results of the MSX α -DC calculations are summarized in Tables VI and VII. First of all, the transitions to Rydberg orbitals show a progressive red shift on increasing the size of M and on replacing hydrogens with methyl groups, following the trend of the vertical ionization potential. Rydberg transitions are expected to be proportional to the ionization potential through the modified hydrogen atom formula 5, if the term value $R/(n - \delta)^2$ is constant

$$E = IP - R/(n - \delta)^2 \quad (5)$$

going down the column of the periodic table, as found for atomic Rydberg transitions³³ (where R is the Rydberg constant, n is the principal quantum number, and δ is the quantum defect that depends on the azimuthal quantum number).

In fact, we found the term value to be almost constant, since the quantum defects δ evaluated from the ionization potentials and the transition energies reported in Tables VI and VII increase by nearly 1 unit on going from one row to the next.⁴⁰ Unfortunately the experimental ionization potential is available only for the Si derivatives. The calculated ionization potentials of silyl and trimethylsilyl radicals are in fairly good agreement with the experimental value, viz., 8.32 ± 0.07 ⁴¹ and 7.03 ± 0.1 eV,⁴² respectively. Thus, the computed Rydberg transition should be accurate enough also for heteroatom-centered radicals. The second point to be noted from the data in Table VI and VII is the existence of both Rydberg and low-lying valence states (in the alkyl radical series the low-lying states are only Rydberg in nature) as well as mixed Rydberg-valence transitions occurring just above the lowest Rydberg transition (ns) in the simplest analogues (H_3M^*).

As regards the simplest heteroatom-centered radicals, i.e., H_3M^* , to our knowledge, there are a recent accurate ab initio MRD-CI calculation⁴³ on H_3Si^* and MSX α calculations⁴⁴ on ionization potentials and electron affinities of H_3Si^* and H_3Ge^* , as well as the electronic spectrum of the silyl⁴⁵ and germyl⁴⁶ radicals obtained by resonance-enhanced multiphoton ionization spectroscopy. In the latter, the spectra obtained in the region of 24 400–27 400 and 23 200–27 000 cm⁻¹ for H_3Si^* and H_3Ge^* , respectively, have been derived from two-photon resonance and were attributed to the np Rydberg transition. For H_3Si^* (C_{3v} sym-

(35) Moc, J.; Latajka, Z.; Ratajczak, H. *Chem. Phys. Lett.* **1986**, *130*, 541; *J. Phys. D: At. Mol. Clusters.* **1986**, *185*; *J. Mol. Struct.* **1986**, *138*, 353.

(36) Gunnarson, O.; Lundqvist, B. I. *Phys. Rev. B* **1976**, *13*, 4274.

(37) Vosko, S. H.; Wilk, L.; Nusair, M. *Can. J. Phys.* **1980**, *58*, 1200.

(38) A reviewer points out that a slightly smaller overlap might provide calculated transition energies even closer to the experimental values; although this might be true, we believe that the generality of the virial ratio approach should be maintained.

(39) MSX α calculations has also been performed on the ethyl radical with the outer sphere centered at the carbon of CH_2 moiety rather than at the barycenter of the radical (cf. Table III). The results indicate that the gap between these two arrangement is about 4000 cm⁻¹, the latter being closer to experimental value.

(40) For example: the δ values for s orbitals are 1.14, 2.00, 3.02, and 3.94 for C, Si, Ge, and Sn, respectively, in H_3M^* and 1.12, 1.99, 2.95, and 3.87 for C, Si, Ge, and Sn, respectively, in $(CH_3)_3M^*$.

(41) Ding, A.; Cassidy, R. A.; Cordis, L. S.; Lampe, F. W. *J. Chem. Phys.* **1985**, *83*, 3426.

(42) Szepes, L.; Baer, T. *J. Am. Chem. Soc.* **1984**, *106*, 273.

(43) Olbrich, G. *Chem. Phys.* **1986**, *101*, 381.

(44) Moc, J.; Latajka, Z.; Ratajczak, H. *J. Mol. Struct.* **1987**, *150*, 189.

(45) Johnson, R. D., III; Hudgens, J. W. *Chem. Phys. Lett.* **1987**, *141*, 163.

(46) Johnson, R. D., III; Tsai, B. P.; Hudgens, J. W. *J. Chem. Phys.* **1988**, *89*, 4558.

Table IV. Vertical Transition Energies (cm⁻¹), Vertical Ionization Potential (eV), and Charge Distributions in the Excited Orbitals for the Isopropyl Radical (\tilde{X}^2A') (Oscillator Strengths Reported in Parentheses)

	exptl	43 435	MSX α -DC ^b	% charge distribution				
				C	H	Me	int	out
² A'(3s)	37 000 ^c	36 944	29 900 (0.174)	1	0	3	34	62
² A'(3p)			34 700 (0.005)	2	0	2	22	74
² A'(3p)	42 000 ^c		35 700 (0.015)	2	0	2	17	79
² A''(3p)		43 435	39 700 (0.001)	1	0	2	7	90
² A'(3d)	48 300 ^c		42 900 (0.063)	1	0	0	12	87
² A'(3d)			43 600 (0.006)	1	0	1	11	87
² A'(3d)			44 800 (0.001)	1	0	1	7	91
² A''(3d)		49 642	46 100 (0.000)	0	0	0	3	97
² A''(3d)			46 500 (0.003)	0	0	1	2	97
² A'(val)	7.69 ^d	57 977	57 200 (0.012)	26	16	48	9	1
IP		7.56	7.4 ^e	57	0	9	32	2

^a From ref 4. ^b The sphere radii are $r_{C\alpha} = 1.7698$, $r_{C\beta} = 1.7242$, $r_H = 1.2482$, and $r_{out} = 5.3277$. ^c From ref 3. ^d From ref 32. ^e SP value; spin-restricted value is 7.1 eV.

Table V. Vertical Transition Energies (cm⁻¹), Vertical Ionization Potentials (eV), and Charge Distributions in the Excited Orbitals for the *tert*-Butyl Radical (\tilde{X}^2A_1) (Oscillator Strengths Reported in Parentheses)

	exptl	SCF ^a	MSX α -DC ^b	% charge distribution			
				C	Me	int	out
² A ₁ (3s)	30 000 ^c	33 619	29 000 (0.069)	2	4	27	67
² A ₁ (3p)	39 500 ^c	38 621	35 500 (0.034)	1	3	20	76
² E(3p)		40 139	38 500 (0.002)	0	3	6	91
² A ₁ (3d)	42 900 ^c	43 125	42 900 (0.011)	1	1	7	91
² E(3d)			43 700 (0.000)	0	1	1	98
² E(3d)			44 700 (0.001)	0	1	1	98
² E(val)		63 380	54 900 (0.025)	28	60	9	3
IP	6.92 ^d	6.73	7.1 ^e	56	12	30	2

^a From ref 4. ^b The sphere radii are $r_{C\alpha} = 1.7491$, $r_{C\beta} = 1.7340$, $r_H = 1.2590$, and $r_{out} = 5.3415$. ^c From ref 3. ^d From ref 32. ^e SP value; spin-restricted value is 6.7 eV.

Table VI. Vertical Transition Energies (cm⁻¹) and Vertical Ionization Potentials (eV) for the H₃M^{*} Radical (\tilde{X}^2A_1) (Oscillator Strengths and Charge Distributions in the Outer Sphere Reported in Parentheses)

	Si ^a		Ge ^b		Sn ^c	
	MSX α -DC	exptl	MSX α -DC	exptl	MSX α -DC	
² A ₁ (ns)	35 500 (0.001, 86)		33 300 (0.001, 79)		32 300 (0.001, 79)	31 300 ^d
² E(np)	45 600 (0.007, 92)		45 300 (0.015, 90)		42 400 (0.012, 94)	43 100
² A ₁ (np)	46 300 (0.008, 92)	48 427 ^e	46 100 (0.008, 94)	47 705 ^f	43 100 (0.004, 95)	43 900
² E(nd)	49 600 (0.014, 97)		50 100 (0.014, 97)		44 500 (0.028, 95)	45 700
² A ₁ (nd)	52 900 (0.000, 99)		52 000 (0.001, 99)		48 400 (0.001, 99)	49 000
² E(nd)	52 700 (0.001, 99)		52 300 (0.001, 99)		48 600 (0.005, 99)	49 200
² E(Ry-val)	37 700 (0.090, 66)		39 100 (0.060, 77)		33 600 (0.100, 64)	35 200
² A ₁ (Ry-val)	40 200 (0.141, 74)		39 400 (0.165, 73)		33 900 (0.219, 64)	35 200
² E(val)	44 000 (0.040, 6)		42 000 (0.037, 7)		38 800 (0.022, 7)	37 400
IP	7.8 ^g	8.32 ^h	7.6 ^g		7.2 ^g	7.3 ^g

^a The spheres radii are $r_{Si} = 2.3486$, $r_H = 1.4082$, and $r_{out} = 4.1578$. ^b The sphere radii are $r_{Ge} = 2.3932$, $r_H = 1.3754$, and $r_{out} = 4.2041$. ^c The sphere radii are $r_{Sn} = 2.6540$, $r_H = 1.4083$, and $r_{out} = 4.5109$. ^d Relativistic calculations. ^e From ref 45. ^f From ref 46. ^g SP value. ^h From ref 41.

Table VII. Vertical Transition Energies (cm⁻¹) and Vertical Ionization Potentials (eV) for the (CH₃)₃M^{*} Radical (\tilde{X}^2A_1) (Oscillator Strengths and Charge Distributions in the Outer Sphere Reported in Parentheses)

	Si ^a	Ge ^b	Sn ^c
² A ₁ (ns)	26 900 (0.017, 64)	26 300 (0.014, 64)	25 800 (0.009, 61)
² E(np)	31 600 (0.107, 64)	30 600 (0.112, 68)	27 600 (0.180, 54)
² A ₁ (np)	32 800 (0.004, 79)	31 400 (0.002, 79)	29 400 (0.005, 68)
² A ₁ (nd)	41 700 (0.001, 95)	40 300 (0.010, 95)	38 900 (0.002, 92)
² E(nd)	42 300 (0.007, 97)	40 800 (0.0008 97)	39 400 (0.001, 95)
² E(nd)	43 400 (0.000, 98)	42 200 (0.0048 98)	40 600 (0.003, 98)
² E(val)	31 500 (0.102, 2)	29 800 (0.053, 2)	24 200 (0.083, 4)
IP	6.7 ^d	6.5 ^d	6.2 ^d

^a The sphere radii are $r_{Si} = 2.4076$, $r_C = 1.7961$, $r_H = 1.2600$, and $r_{out} = 6.0087$. ^b The sphere radii are $r_{Ge} = 2.4404$, $r_C = 1.7988$, $r_H = 1.2633$, and $r_{out} = 6.0329$. ^c The sphere radii are $r_{Sn} = 2.7876$, $r_C = 1.8163$, $r_H = 1.2649$, and $r_{out} = 6.4434$. ^d SP value.

metry), the ²E valence excitation and the [$\tilde{X}^2A_1 \rightarrow \tilde{2}A_1(4s)$, ²A₁(4p)] excitation energies are underestimated by about 2000 and 5000 cm⁻¹, respectively, as compared to those from MRD-CI calculations. However, the experimental Rydberg excitation energy (48 427 cm⁻¹) for the [$\tilde{X}^2A_1 \rightarrow \tilde{2}A_1(4p)$] transition is

half-way between the MSX α -DC (46 300 cm⁻¹) and ab initio CI (50 708 cm⁻¹) value. In contrast with alkyl radicals, transitions to mixed Rydberg-valence orbitals occur at low energy, just above the energy of the [$\tilde{X}^2A_1 \rightarrow \tilde{2}A_1(4s)$] transition. The computed oscillator strengths suggest that these transitions should be the most intense in the one-photon optical absorption spectrum. The charge density analysis shows that the mixed Rydberg-valence orbitals derive from the interaction of the Si-H antibonding MOs, having large participation of the d orbitals on Si atom (50%), with s, p, and d orbitals in the ²A₁ state and p and d Rydberg orbitals in the ²E state. Mixed Rydberg-valence transitions were also found at MRD-CI level in the same spectral region, viz., between 4s and 4p Rydberg transitions. The ²E transition occurs about 2000 cm⁻¹ above the 4s Rydberg transition in both the MSX α -DC and the MRD-CI (44 189 cm⁻¹) approaches, whereas the ²A₁ transition occurs 4700 cm⁻¹ in the MSX α -DC and 8800 cm⁻¹ in the MRD-CI (50 626 cm⁻¹) approaches above the 4s Rydberg transition. This discrepancy could be due to the small contribution of valence orbitals in the ²A₁ state at MRD-CI level. The small red shift experimentally observed for the $\tilde{X}^2A_1 \rightarrow np$ transition on going from H₃Si^{*} to H₃Ge^{*} (47 705 cm⁻¹) was also reproduced by the present MSX α -DC calculations. Therefore, the lowest excitation energies computed with the MSX α -DC approach are

in good agreement with ab initio MRD-CI calculation and available spectroscopic data as found for the methyl and *tert*-butyl radicals.

As far as the vertical ionization potential is concerned, it is appreciably underestimated for H₃Si^{*}, the difference of 0.52 eV with experiment (8.32 eV) being larger than that obtained in the MSX α approach^{44,47} by Ratajczak and co-workers (8.0 eV) and in MRD-CI (8.52 eV) calculations. It is evident that the accuracy of the MSX α -DC approach for estimating vertical ionization potentials is slightly worse than that for valence and Rydberg excitations. This is probably due to underestimation of the electron correlation energy that should be more important in computing ionization potentials since in the final state the number of correlated electrons decreases by 1 unit. A more correlated exchange-correlation potential could in principle improve the agreement with experiment.

As far as the H₃Sn^{*} radical is concerned, neither experimental nor theoretical data are available; however, we utilize H₃Sn^{*} to establish the influence in stannyl radicals of relativistic effects, which increase with the atomic number. Table VI shows that the relativistic effects do not appreciably affect the electronic transitions, the relativistic energy shifts being about 1000 cm⁻¹.

As far as the alkyl derivatives of group 14 heteroatom-centered radicals are concerned, the optical absorption spectra of (alkyl)₃M^{*} (M = Si, Ge, Sn) have been recorded over the last few years,^{9,48,49} although assignments to specific transitions have not been attempted. Having established the reliability of the MSX α -DC approach, we assign these spectra on the basis of the excitation energies computed for the model compounds (CH₃)₃M^{*} (C_{3v} symmetry). The optical absorption spectra of all (alkyl)₃M^{*} radicals show a strong band at frequencies higher than 30 000 cm⁻¹. The MSX α -DC calculations assign this strong band to the transition to the np Rydberg orbital. This transition is forbidden in planar radicals such as methyl, but it becomes the most intense transition upon pyramidalization of the radical center. Furthermore, the spectra of these radicals show a weaker band/shoulder at lower frequencies, which is red shifted as the size of M increases. For the Si derivative the optical spectrum shows a weak symmetric band with a maximum at 25 800 cm⁻¹, which we assign, according to the MSX α -DC results, to the 4s Rydberg transition. The MSX α -DC calculations indicate that one feature in this spectral region for Ge and Sn derivatives could be attributed to the valence transition from the MO localized at the C-M bond to the SOMO. This behavior can be attributed to the great decrease of electronegativity along the series M = C \gg Si \approx Ge $>$ Sn,⁵⁰ which weakens the C-M bond with respect to the C-C

bond. The energy of the valence transition decreases by 24 000–30 000 cm⁻¹ on going from carbon- to heteroatom-centered radicals, being evaluated in the range of ns and np Rydberg transitions with intermediate intensity with respect to them, whereas in alkyl radicals it occurs at higher energy than the 3d Rydberg transition. Since the red shift for the valence transition is more pronounced than for the Rydberg ones on changing the heteroatom, the valence transition, which occurs just below the 4p Rydberg transition in the Si derivative, is red shifted toward the 5s transition in the Ge derivative and becomes the lowest transition in the Sn derivative. This theoretical sequence has its counterpart in the absorption spectra. In particular, a well-resolved shoulder is present at 29 300 cm⁻¹ in the absorption spectrum of Bu₃Ge^{*}. In the absorption spectrum of Bu₃Sn^{*} an asymmetric band is present with a maximum at 26 100 cm⁻¹; this band can effectively be due to the overlapping of the valence and 6s Rydberg transitions.

Conclusions

The MSX α method has been shown to be a powerful tool for assigning the absorption spectra of radicals, if the Norman procedure and the virial ratio criterion are utilized to determine the sphere radii and the double-counting correction for overlap is applied in normalizing the MSX α wave functions. The method reproduces very well the spectral features that are due to either Rydberg or valence transition in highly symmetric radicals, the accuracy being comparable to that obtained by accurate ab initio CI calculations. The agreement with experiment is slightly worse when the radical center is not symmetrically substituted; nevertheless, the experimental trends are reproduced. This shortcoming could not be important, if one keeps in mind that the effect to be investigated can be clearly and uniquely identified by studying symmetric systems. However, MSX α calculations of partitioned clusters⁵¹ that, in theory, should improve the agreement with experiment in asymmetric compounds are in progress.⁵² Furthermore, the small computational effort required for higher atomic number elements and large molecules makes this method more attractive.

Finally, it is worth emphasizing that while in closed-shell molecules the transitions normally observed in the visible and ultraviolet regions are totally within the valence shell, in free radicals the situation is more complicated, the reason being the existence of low-lying Rydberg orbitals that, in molecules, usually occur in the vacuum ultraviolet region. Therefore, knowledge of a specific transition involved in reactive intermediates will be of great importance in the development of the reaction paths induced by two-photon laser excitation.⁵³

Acknowledgment. We thank a reviewer for some constructive suggestions. Financial support from Progetto Finalizzato Chimica Fine II (CNR) is gratefully acknowledged.

(47) It is worth noting that the Rydberg excitation [$\tilde{X}^2A_1 \rightarrow ^2A_1(4s)$] and the ²E valence transition are underestimated by about 7000 cm⁻¹ from MRD-CI calculations. Probably, the small radii used in these calculations improve the estimate of the ionization potential, whereas excitation energies seem to be more sensible to the type of procedure employed in the MSX α calculation.

(48) Shimo, N.; Nakashima, N.; Yoshihara, K. *Chem. Phys. Lett.* **1986**, *125*, 303.

(49) Chatgililoglu, C.; Scaiano, J. C.; Ingold, K. U. *Organometallics* **1982**, *1*, 466.

(50) Allred, A. L.; Rochow, E. G. *J. Inorg. Nucl. Chem.* **1958**, *5*, 264.

(51) Kjellander, R. *Chem. Phys.* **1976**, *12*, 469.

(52) Guerra, M. Unpublished results.

(53) For a recent review see: Scaiano, J. C.; Johnston, L. J.; McGimpsey, W. G.; Weir, D. *Acc. Chem. Res.* **1988**, *21*, 22.